Structure and interactions of ultracold Yb ions and Rb atoms

H. D. L. Lamb,[*] J. F. McCann,[†] and B. M. McLaughlin[‡]

Centre for Theoretical Atomic, Molecular and Optical Physics, School of Mathematics and Physics, Queen's University Belfast,
Belfast BT7 1NN, United Kingdom

J. Goold

Clarendon Laboratory, University of Oxford, Oxford, United Kingdom and Department of Physics, University College Cork, Cork, Ireland

N. Wells and I. Lane

Innovative Molecular Materials Group, School of Chemistry and Chemical Engineering, Queen's University Belfast,
Belfast BT9 5AG, United Kingdom

In order to study ultracold charge-transfer processes in hybrid atom-ion traps, we have mapped out the potential-energy curves and molecular parameters for several low-lying states of the Rb, Yb$^+$ system. We employ both a multireference configuration interaction and a full configuration interaction (FCI) approach. Turning points, crossing points, potential minima, and spectroscopic molecular constants are obtained for the lowest five molecular states. Long-range parameters, including the dispersion coefficients, are estimated from our *ab initio* data. The separated-atom ionization potentials and atomic polarizability of the ytterbium atom ($\alpha_d = 128.4$ atomic units) are in good agreement with experiment and previous calculations. We present some dynamical calculations for (adiabatic) scattering lengths for the two lowest (Yb, Rb$^+$) channels that were carried out in our work. However, we find that the pseudopotential approximation is rather limited in validity and only applies to nK temperatures. The adiabatic scattering lengths for both the triplet and singlet channels indicate that both are large and negative in the FCI approximation.

PACS number(s): 34.50.Cx

I. INTRODUCTION

As a gas is cooled down towards μK temperatures, the quantum nature of the interactions begins to dominate. With increasing de Broglie wavelength, the long-range tail of the potential plays a vital role in determining the nature of the interactions, in particular whether the elastic pairwise interaction is, in the limit of zero temperature, attractive or repulsive [1,2]. The lower the incident energy of the ion-atom pair is, the larger the distances are for which these potentials influence the phase shift. This is critical in terms of the ultracold regime as to whether cooling, trapping, and degeneracy can occur. It is extremely important in view of potential applications in exploring the fundamental process of ultracold charge transfer [3–6].

Interest has developed in expanding the range of quantum systems that can be trapped and manipulated on the quantum scale. Hybrid ion-atom systems are of great interest [7] since these are inherently strongly interacting systems with a longer-range potential and inelastic processes can be studied. Recently, these systems have been explored considering two-body collisions, in which both collision partners are translationally cold [8], and on the many-body level [9], where the sympathetic cooling of the ion with ultracold atoms was observed. The study of these systems in the quantum regime can be applied to hybrid atom-ion devices [10] and in addressing fundamental many-body effects of ionic impurities,

such as mesoscopic molecule formation [11] and density fluctuations [12]. These devices also afford a unique opportunity to study reactive collisions (ultracold chemistry) under controlled conditions, for example, when external electric fields can be applied to modify the reaction rates and cross sections [9]. Unlike binary cold collisions between ground-state neutral atoms, which are only elastic or inelastic in nature, reactive collisions (charge transfer) are a feature of Yb ions immersed in a gas of trapped alkali-metal atoms as the products Yb + Rb$^+$ are the thermodynamically favored species. Consequently, curve crossings between electronic states, again absent in the neutral systems studied to date, can play a significant role in determining the collision dynamics.

Ultracold neutral atom interactions are characterized by pure s-wave scattering mediated at long range by the dispersion forces [13]. Conversely, a bare ion creates a polarization force directly, and hence the effective cross section is larger, with significant contributions from higher-order partial waves [14]. Indeed, the usual effective range expansion is modified by logarithmic terms in the wave-number expansion [15]. In the last few years theoretical studies of ultracold atom-ion collisions included the investigation of the occurrence of magnetic Feshbach resonances with a view to examining the tunability of the atom-ion interaction focusing on the specific ^{40}Ca$^+$-Na system [16] and calculations of the single-channel scattering properties of the Ba$^+$ ion with the Rb neutral atom [17], which suggest the possibility of sympathetic cooling of the barium ion by the buffer gas of ultracold rubidium atoms with a considerable efficiency.

In recent experiments [8,9,18], a single trapped ion of ^{174}Yb$^+$ in a Paul trap was immersed in a condensate of neutral ^{87}Rb atoms confined in a magneto-optical trap. A study of

---

[*]hlamb01@qub.ac.uk.

[†]j.f.mccann@qub.ac.uk

[‡]b.mclaughlin@qub.ac.uk

charge-transfer cross sections showed that the simple classical Langevin model was inadequate to explain the reaction rates [9]. However, very little is known about the microscopic ultracold binary interactions between this ion and the rubidium atom. In particular, the potential-energy curves and couplings are not known with any accuracy. Thus the experimental study of the quantum coherence of charge transfer [9] was based on schematics of the energy curves. This prompted our in-depth investigations. Our initial aim was to map the potential-energy curves to establish the adiabatic states and the static properties of the molecular ion, in particular the turning points, potential minima, and crossing points of the lowest molecular energies. In addition to this, the dissociation energies and molecular constants would provide useful spectroscopic data for further investigation. We have made a preliminary estimation of the pseudopotential which approximates the ultracold interaction. This information is of great importance for modeling ultracold charge transfer, in particular the quantum character of chemical reactivity, and thus developing insights into ultracold quantum controlled chemistry, for example, when external fields are applied to influence the reaction rates and reaction channels [9]. Of course, the presence of a bare charge in a dilute gas exposes many-body physics features such as exciton and polariton dynamics, which are also of great interest. It is also of great interest for laser manipulation of the collision to prevent losses through charge transfer or create translationally cold trapped molecular ions via photoassociation.

II. ELECTRONIC STRUCTURE CALCULATION

Beyond the calculation of ionization potentials and dissociation energies, one of the more challenging tasks for a quantum chemistry package is the calculation of polarizabilities and dispersion forces. Since these terms dominate at asymptotic long range and low energies, their accuracy is paramount in obtaining a solid foundation for scattering calculations [19]. In atomic units, the asymptotic singly charged ion-atom potential has the form [13,14]

$$V(R) = V_\infty - \frac{1}{2}\left[\frac{\alpha_d}{R^4} + \frac{C_6}{R^6} + \frac{C_8}{R^8}\right], \quad (1)$$

where α_d is the dipole polarizability of the neutral atom and where C_6 and C_8 are, respectively, the quadrupole and octupole polarizabilities and V_∞ is the asymptotic limit (ionization potential). R is the ion-atom internuclear separation. Of course, the ionization potential and the other coefficients will depend on the electronic configuration and thus on the electronic state in question. The primary interest, for cold-atom physics, is the ground state. However, for temperatures in the mK regime, the excited states have an important role in energy exchanges through collisions. A recent review of existing theoretical methods for ground-state polarizability discusses their relevance to cold-atom physics [19]. Calculations of polarizability for molecules with heavy atoms, even restricting interest to the ground state, become increasingly difficult, partly because of relativistic corrections. However, as is the case of Rb, electron correlation is, in practice, more problematic. For example, a basic nonrelativistic Hartree-Fock calculation [20] gives $\alpha_d \approx 522$ a.u. It requires the power of the CCSD(T) (coupled-cluster single and double (triple)

excitations) expansions [20] to account fully for correlation. The CCSD(T) method gives $\alpha_d \approx 352$ a.u. (nonrelativistic), while relativistic corrections take the value to $\alpha_d \approx 324$ a.u. At this point, the theory is consistent with experiment: 319 ± 6 [21]. However, excited-state calculations are more problematic.

In our approach we employed the MOLPRO [22] suite of *ab initio* quantum chemistry codes (release MOLPRO 2010.1) to perform all the calculations for this diatomic system (Rb, Yb)$^+$ to obtain the potential-energy curves (PECs) as a function of bond length. We used a combination of multireference configuration interaction (MRCI) and full configuration interaction (FCI) approximations. The *ab initio* potential-energy curves for this diatomic system are calculated using effective core potentials (ECP) as a basis set for each atom, which allows for scalar-relativistic effects to be included explicitly. The scalar-relativistic effects are included by adding the corresponding terms of the Douglas-Kroll Hamiltonian to the one-electron integrals. For the short-range interactions for the molecular electronic states we used the nonrelativistic complete-active-space self-consistent field (CASSCF)–MRCI method [23–26] within the MOLPRO [22] *ab initio* quantum chemistry suite of codes.

We used the Stuttgart basis sets and ECPs with core-polarization potentials (CPPs) for Rb and Yb, the ECP68MDF potential for Yb and the ECP36SDF potential for Rb, respectively. The inner-shell electrons are modeled using these effective core potentials for ytterbium (ECP68MDF) [27] and for rubidium (ECP36SDF) [28,29]. We started at a bond separation of $R = 30a_0$ and moved into $R = 5a_0$. At $R = 30a_0$, we perform a self-consistent-field Hartree-Fock (SCF-HF) calculation on the closed-shell YbRb molecular ion system to obtain a starting wave function. This is the starting configuration for the multireference configuration-interaction MRCI calculation performed in the appropriate molecular symmetry group. We used an active space of $\{6a_1, 3b_1, 3b_2, 0a_2\}$ in the C_{2v} Abelian point group with no closed orbitals. We then perform a multiconfiguration self-consistent field calculation (MCSCF). The MCSCF calculation was performed on the lowest five electronic states. These results were used as the initial wave-function set for a MRCI calculation to capture the dynamic electron correlation.

Only the valence shells were included in the determination of the electronic correlation energy. As a test of the basis set employed, we conducted equivalent calculations on the neutral YbRb molecule, yielding values as expected, consistent with those of Meyer and Bohn [30].

The MRCI calculations do not explicitly include relativistic effects, although this is not important for the entrance collision channel or the lower Yb (^1S) + Rb$^+$ (^1S) asymptote as all the molecular states formed are of Σ^+ symmetry. This is borne out by the calculated energy of the asymptotic energies of the $a\,^3\Sigma^+$ and $A\,^1\Sigma^+$ states (Table I). The asymptotes for the higher $^3\Pi$ and $^3\Sigma^+$ states correlate to the Yb ($6s6p\,^3P^o$) + Rb$^+$ ($4p^6\,^1S$) atomic products. The multiplet and its associated fine-structure splitting in the triplet (Yb: $^3P^o_{0,1,2}$) is considerable: ~ 0.3 eV. Only a fully relativistic treatment can accurately account for the spin-orbit interaction. In a magnetic trap, of course, the Zeeman splitting and hyperfine structure complicates matters further. Nonetheless, in our first analysis of this

TABLE I. Comparison between the experimental and calculated molecular asymptotes. The experimental asymptotes are derived from ionization potentials [31–34]. The calculated asymptotes are obtained by the fit (2) using the LEVEL code [35].

Molecular symmetry	Estimated $E_\infty^{(i)}$ (eV)	Experimental asymptotic limit (eV)	ΔE difference (eV)	ΔE difference (%)
$X\,^1\Sigma^+$	0	0	0	
$a\,^3\Sigma^+$	2.036	2.076	0.040	1.93
$A\,^1\Sigma^+$	2.036	2.076	0.040	1.93
$b\,^3\Pi$	2.045	2.143	0.089	4.15
$b\,^3\Sigma^+$	2.050	2.143	0.093	4.34

novel system, we can confidently say that a curve crossing will take place between the $A\,^1\Sigma^+$ and $b\,^3\Pi$ states, although at an energy above the Yb$^+$ (^2S) + Rb (^2S) asymptote, as shown in Fig. 1. Such a crossing will facilitate a charge-exchange reaction, as observed in experiment at mK temperatures [8,9]. We have estimated the molecular constants for the four states that support bound rovibrational states. These constants are defined by the usual expression for electronic state (channel) i with asymptotic energy $E_\infty^{(i)}$,

$$
\begin{aligned}
E(i,v,J) = {} & E_\infty^{(i)} - D_e^{(i)} + \hbar\omega_e^{(i)}\left(v + \tfrac{1}{2}\right) - \hbar\omega_e^{(i)}x_e\left(v + \tfrac{1}{2}\right)^2 \\
& + B^{(i)}J(J+1) - D^{(i)}J^2(J+1)^2.
\end{aligned}
\tag{2}
$$

All the constants were derived from the electronic potentials and were calculated using the LEVEL [35] program (version 8.0). The values are presented in Table II.
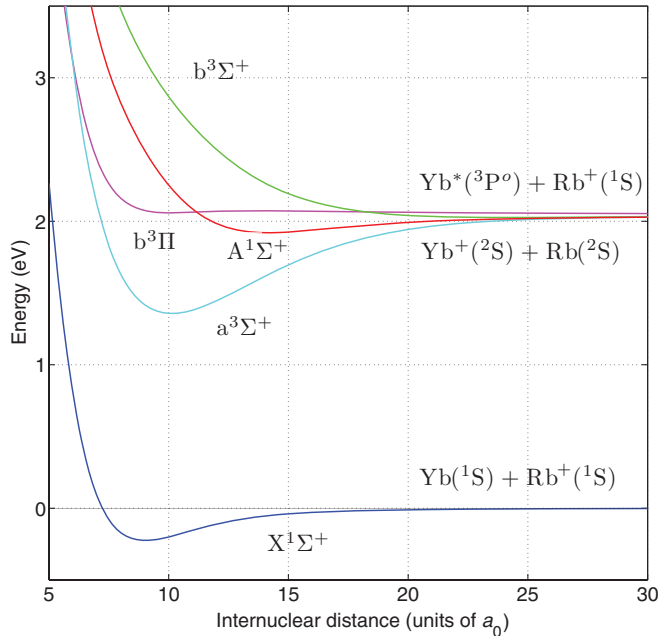

FIG. 1. (Color online) Relative electronic energies for the molecular ion YbRb$^+$ as a function of internuclear distance R (MRCI approximation). The $X\,^1\Sigma^+$ ground state is the Rb$^+$ channel, while the lowest-energy ionic ytterbium states, the triplet $a\,^3\Sigma^+$ and singlet $A\,^1\Sigma^+$ pair, are nearly degenerate with the excited charge-transfer channels: Rb$^+$ + Yb*.

A. Scattering length calculation

In the adiabatic approximation the dynamics occur on decoupled, centrally symmetric potential-energy curves. Using conventional notation, we let E denote the collision energy in the center-of-mass frame and m_i and m_a the ion and atom masses, respectively. Then, the reduced mass is $\mu = m_i m_a/(m_i + m_a)$. Using atomic units, unless otherwise stated, the molecular channel i, $k^2 = 2\mu(E - E_\infty^{(i)}) \geqslant 0$ is the relative wave number squared. The mean-square wave number has the equivalent temperature $T = \hbar^2\langle k^2\rangle/(3k_B\mu)$, where k_B is the Boltzmann constant. For this ^{174}Yb$^+$, ^{87}Rb system, we have k (a.u.) $\approx \sqrt{T(\text{K})}$. From Fig. 2 one sees that the upper limit of the energy range, $k = 10^{-4}$ a.u., corresponds to $T \approx 10$ nK.

The radial Schrödinger equation for the s-wave in the channel or potential i is then

$$
\left[\frac{d^2}{dR^2} + k^2 - 2\mu V_i(R)\right]\chi_i(k,R) = 0,
\tag{3}
$$

where $V_i(R) \sim -\alpha_d/(2R^4)$ as $R \to \infty$. Then the phase shift $\delta_i(k)$ has its usual definition,

$$
\chi_i(k,R) \sim \sin[kR + \delta_i(k)], \quad R \to \infty.
\tag{4}
$$

At ultracold temperatures, $k \to 0$, the effective range expansion for the s wave [15], takes the form

$$
\begin{aligned}
k\cot\delta_i(k) = {} & -\frac{1}{a_s} + \frac{\pi\mu\alpha_d}{3a_s^2}k \\
& + \frac{4\mu\alpha_d}{3a_s}k^2\ln\left(\frac{k}{4}\sqrt{\mu\alpha_d}\right) + O(k^2).
\end{aligned}
\tag{5}
$$

We note the logarithmic terms in k as opposed to the usual quadratic term for a short-range force. Clearly, at zero

TABLE II. Molecular constants for the four lowest states supporting rovibrational bound states in the MRCI approximations. The equilibrium bond length r_e is in atomic units, the dissociation energy D_e is in eV, and both were obtained from the *ab initio* data. The rovibrational constants defined in Eq. (2) are in cm^{-1}. Note that the $b\,^3\Sigma^+$ state is repulsive.

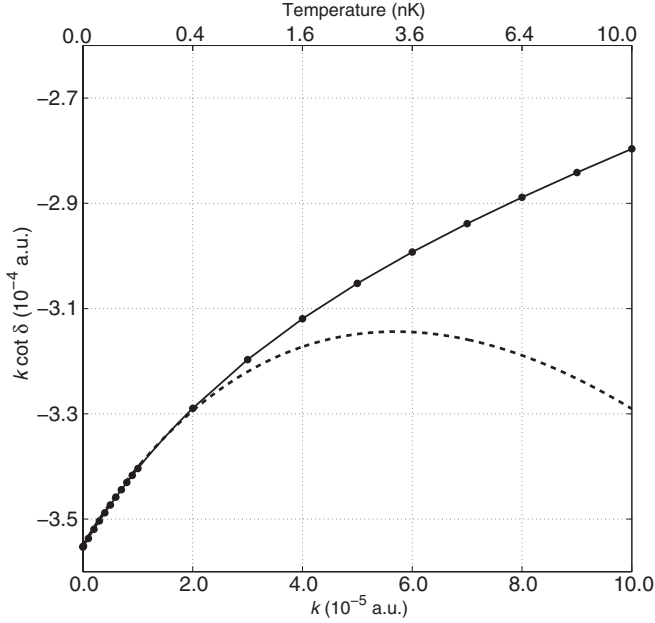| Molecular symmetry	r_e (units of a_0)	ω_e (cm^{-1})	$\omega_e x_e$ (cm^{-1})	B (cm^{-1})	D (10^{-9} cm^{-1})	D_e (eV)
$X\,^1\Sigma^+$	9.031	33.77	−0.22	0.012 73	7.0047	0.2202
$a\,^3\Sigma^+$	10.142	34.94	0.04	0.010 10	3.3843	0.6653
$A\,^1\Sigma^+$	14.362	16.807	0.38	0.005 05	2.1440	0.1085
$b\,^3\Pi$	10.108	15.24	−0.21	0.001 02	16.812	0.0061

FIG. 2. The effective-range function, $k\cot\delta(k)$, in the limit of low energy as a function of the relative wave number k and equivalent temperature, for the $X\,{}^1\Sigma^+$ state in the MRCI approximation. The solid line is the value obtain by numerical integration. The dashed curve displays the low-temperate expansion (5). For this system, it is clear that replacing the scattering by a temperature-independent pseudo-potential (7) is only valid in the nK regime.

temperature, the s-wave scattering length a_s has the usual expression,

$$a_{i,s} = \lim_{k\to 0} -\frac{\tan\delta_i(k)}{k}. \qquad (6)$$

The significance of the scattering length for ultracold gases is as a strength parameter for a contact two-body pseudopotential that can, in turn, be used in the many-body Hamiltonian appropriate for an ion embedded in a cloud of cold atoms. Thus, for channel i and ion-atom separation $\vec{R}$, we have the zero-temperature pseudopotential [36] (operating to the right):

$$U_i(\vec{R}) = \frac{2\pi\hbar^2}{\mu} a_{i,s}\,\delta(\vec{R})\frac{\partial}{\partial R}R\,. \qquad (7)$$

In general, the pseudopotential can be made energy dependent: $a_{i,s}$ is replaced by $a(k)$, where k is the wave number. At distances near the equilibrium bond length r_e the interaction between the ion charge and the dipole moment in the atom results in a deep potential well for which the thermal de Broglie wavelength λ is small, with the potential slowly varying, and a semiclassical approximation is justified. At long range, where the dipole potential is the dominant term, the radial Schrödinger equation (3) can be solved in closed analytic form. Connecting the exact asymptotic solution with the semiclassical approximation at a *matching distance R_c* gives the phase shift in terms of a simple quadrature [37,38]. This, in turn, yields an elegant and simple expression for the scattering length,

$$a_s = -\sqrt{\mu\alpha_d}\,\tan\left(\Phi - \frac{\pi}{4}\right), \qquad (8)$$

where

$$\Phi = \int_{R_0}^{\infty} \sqrt{-2\mu V(R)}\,dR, \qquad (9)$$

with R_0 being the zero-energy classical turning point, i.e., the smallest value for the solution of $V(R_0) = 0$. The phase (9) is the accumulation of the inner (semiclassical) phase as far as the matching radius R_c and the outer (asymptotic) phase beyond the matching radius in the region where the potential is approximately a pure dipole. This can be simply written as [37,38] $\Phi = \Phi_< + \Phi_>$, where

$$\Phi_< = \int_{R_0}^{R_c} \sqrt{-2\mu V(R)}dR, \quad \Phi_> = \sqrt{\mu\alpha_d}\frac{1}{R_c}. \qquad (10)$$

In accordance with Levinson's theorem, the phase Φ passes through many cycles of π at the threshold energy. For a dipole potential and within the semiclassical approximation, the number of bound states is given by

$$n_s = \text{int}[\Phi/\pi - 3/4] + 1. \qquad (11)$$

The large, but uncertain, value of the phase leads one to the conjecture [37] that there is equal likelihood that the scattering length is positive or negative, and indeed, it may be infinitely large in magnitude. This sensitivity of scattering length to phase shift, which, in turn, depends on the interatomic potential amplified by the large reduced mass, means that obtaining accurate and reliable theoretical estimates of the scattering length is extremely difficult. Nonetheless, one of the aims of this paper is to make a first estimate of these values.

III. RESULTS

A. Ground state

First, we consider the $X\,{}^1\Sigma^+$ electronic potential corresponding to the separated ion-atom asymptotic channel, Rb$^+$ $(4p^6\,{}^1S)$ + Yb $(6s^2\,{}^1S)$. In this case, the ytterbium atom experiences the long-range single charge of the Rb ion, and the electronic potential has the leading-order term of order R^{-4}. As a test of the accuracy of the electronic energy curve we obtained, we estimated the ytterbium polarizability by curve fitting the potential to $-\frac{1}{2}\alpha_d R^{-4}$ at values of $R > 30$ a.u. We used a least-squares fit over 15 points using a constant and R^{-4} as independent variables for which we computed the coefficients corresponding, respectively, to the ionization energy and the polarizability of the atomic species. For the ground electronic state $X\,{}^1\Sigma^+$, which corresponds asymptotically to Rb$^+$ $(4p^6\,{}^1S)$ and neutral Yb$(6s^2\,{}^1S)$, the hyperpolarizability terms have a small contribution, so at internuclear distances beyond $30a_0$ they may be neglected. From this approach we find estimates of the polarizability of ytterbium $\alpha_d \approx 128.5$ in both MRCI and FCI approximations, which are in suitable agreement with results from previous investigations; see Table III.

In order to obtain estimates for the scattering length, we performed numerical integration of the radial Schrödinger equation (3) to determine the phase shift using the Runge-Kutta method along with a numerical quadrature (Simpson's rule) for the semiclassical approximation. The numerical integration was initiated just to the left of the classical turning point and integrated outwards to fit to the form (4).

The phase shift was determined by numerically integrating the radial Scrödinger equation (3) using a simple fourth-order Runge-Kutta scheme starting within the classically forbidden region out to the matching radius $R_c \sim 37a_0$. This distance was sufficiently large enough to ensure that beyond this value the potential is then suitably represented by the multipole expansion (1). The leading-order dipole term with the value $\alpha_d = 128.4894$ gave $n_s = 155$ bound states for the MRCI calculation. The full configuration interaction calculation gives $n_s = 155$. From this we find a large negative scattering length, indicating the presence of a virtual bound state at $E = (2\mu a_s^2)^{-1}$. Our calculated polarizability (see Table III) falls within the range of previous theoretical and experimental results.

The de Broglie wavelength increases as $k \to 0$. For $k < 10^{-3}$ ($T \lesssim 1\,\mu$K) the collisional properties are determined by s-wave scattering. We are already well into the nK regime when $k = 10^{-8}$, for which convergence of the phase shift to its value in the low-energy limit, to reasonable accuracy, can be assumed. Integration is carried out to a distance for which the long-range dispersion potentials have a negligible effect on the phase, $k^2 \gg \mu\alpha_d/R^4$. The method of extrapolation of the zero-energy wave function is less computationally expensive and can be used as a test against the results for very low energy scattering. The numerically obtained low-energy s-wave phase shifts are in good agreement with those from the low-energy phase-shift expansion (5) using the semiclassical scattering length ($a_{SC} = 2816.7$ in the MRCI approximations), as illustrated in Fig. 2 for the range of $ka_s \lesssim 0.3$.

The variation in the effective scattering length,

$$a(k) = -\frac{\tan\delta(k)}{k}, \tag{12}$$

with relative wave number k, is shown in Fig. 3. We also consider a comparison with the linear expansion of Eq. (5) via the binomial approximation, which gives, in this case,

$$a(k) = a_s \left(1 - \frac{\pi\mu\alpha_d}{3a_s}k\right)^{-1} \approx a_s \left(1 + \frac{\pi\mu\alpha_d}{3a_s}k\right). \tag{13}$$

In Fig. 3 the numerical calculation (solid line with circles) deviates from both the linear and nonlinear expansions, even at these extremely low temperatures. Based on these preliminary calculations, current experiments, operating in the μK range, would have great difficulty in estimating the scattering length. The linear approximation is adequate for temperatures
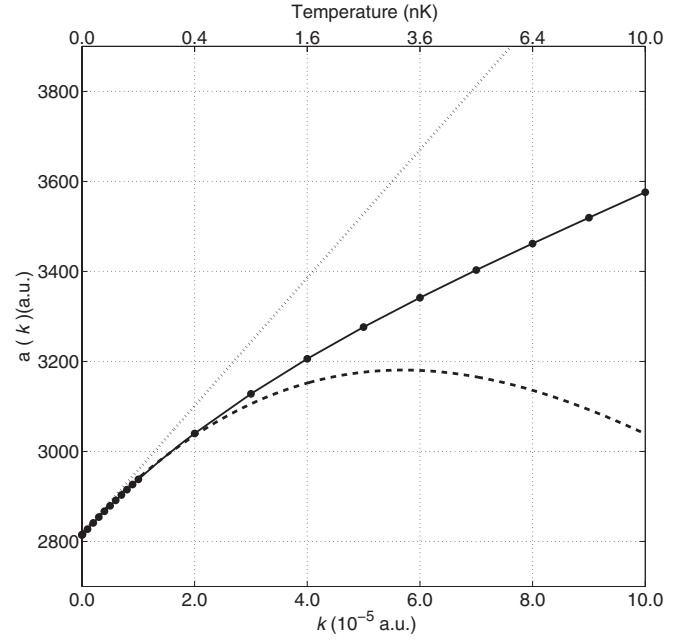

FIG. 3. The energy-dependent scattering length $a(k)$, defined by Eq. (12), for the ground-state potential curve ($X\,^1\Sigma^+$) in the MRCI approximations. The solid curve is the result of numerical integration, the dotted line is the linear approximation (13), and the dashed curve is the nonlinear expansion (5). Even over this ultracold (nK) temperature range the variation of the effective scattering length is significant.

$T < 1$ nK, while expansion (5) breaks down at $T = 1$ nK, as higher-order terms then become significant.

B. Excited states

In ion-trap experiments, the primary interaction will be the Yb$^+$($6s\,^2S$) ion colliding with the neutral Rb ($5s\,^2S$), which may occur in the $A\,^1\Sigma^+$ singlet or the $a\,^3\Sigma^+$ triplet state. We see (Fig. 1) that the triplet has a lower minimum and shorter bond length and because of the statistical weight is the more important channel. In the separated-atom limit, this channel lies 2.036 eV above the ground state, corresponding to the difference in ionization potentials of Rb and Yb. Considering the long-range numerical values of the potential, we find that the hyperpolarizabilities in the multipole expansion (1) need to be taken into account. Little spectroscopic information about quadrupole or octupole moments for the heavier alkali-metal

TABLE III. Static electric-dipole polarizability α_d (a.u.) for the ground state of Yb ($6s^2\,^1S_0$) compared with previous experimental and theoretical work.

α_d	Comment
128.5	This work (MRCI)
128.4	This work (FCI)
141 ± 6	Dzuba and Derevianko; configuration-interaction method and many-body perturbation theory (CI + MBPT) [39]
136.4 ± 4.0	Experimental data [40]
157.3	Chu et al.; density functional theory [41]
141 ± 35	Linear response method [42]

TABLE IV. Molecular constants and multipole coefficients obtained from the *ab initio* data for the lowest three states of YbRb$^+$ in the MRCI approximation. The equilibrium bond length r_e and the dissociation energy D_e were obtained using a spline fit to the data. C_8 and E_∞ were obtained using a least-squares fit. The scattering length given by a_s is in atomic units.

Molecular symmetry	r_e (a_0)	D_e (eV)	C_8 (10^8 a.u.)	E_∞ (eV)	a_s (a_0)
$X\,^1\Sigma^+$	9.024	0.2244		0	2815
$A\,^1\Sigma^+$	14.179	0.1161	1.770	2.036	6766
$a\,^3\Sigma^+$	10.135	0.6785	1.786	2.036	9646

TABLE V. Molecular constants and multipole coefficients obtained from the *ab initio* data for the lowest three states of YbRb$^+$ in the FCI approximation. The equilibrium bond length r_e and the dissociation energy D_e were obtained using a spline fit to the data. C_8 and E_∞ were obtained using a least-squares fit. The scattering length given by a_s is in atomic units.

Molecular symmetry	r_e (a_0)	D_e (eV)	C_8 (10^8 a.u.)	E_∞ (eV)	a_s (a_0)
$X\,^1\Sigma^+$	9.031	0.2227		0	$-11\,594$
$A\,^1\Sigma^+$	14.184	0.1150	0.7020	2.035	$-59\,036$
$a\,^3\Sigma^+$	10.134	0.6776	1.2172	2.035	-3606

atoms exists as it is very difficult to precisely measure the oscillator strengths. For the higher-order multipole terms we obtained solutions first by fitting the data to Eq. (1). In this case, we chose to fix the dipole and quadrupole polarizabilities by their experimental values $\alpha_d = 319.2$ a.u [21] and $C_6 = 6480$ a.u. [43], respectively. We then fitted to our data points to obtain C_8 using a least-squares fitting procedure. The results in the MRCI and FCI approximations are given in Tables IV and V, respectively. In both cases (MRCI and FCI) the scattering length a_s for the ground electronic state $X\,^1\Sigma^+$ is shown. The dipole polarizabilities for the ground state of Yb from the MRCI and FCI approximations are, respectively, 128.5 and 128.4 (cf. Table III).

For two electrons outside a closed shell one expects both the MRCI and FCI results to be in suitable agreement with each other. Figure 1 illustrates only the MRCI results as on the scale shown the FCI results are identical. From our *ab initio* results, while it is seen that the equilibrium bond distance r_e and the dissociation energy D_e are practically identical in the MRCI and FCI approximations, the scattering lengths are widely different. This we attribute to the difficulty of accurately obtaining the dispersion coefficients from the long-range tail of the potential (1) in both approximations, which are subsequently used in numerically solving the radial Schrödinger equation (3) for the phase shift and corresponding scattering length. We illustrate this fact with the values tabulated in Tables IV and V for the scattering length.

IV. CONCLUSIONS

We have investigated the electronic structure of the low-lying states of the diatomic molecular ionic system containing a ytterbium ion and a rubidium atom, with relevance to ultracold chemistry, in particular, charge-transfer processes involving Yb ions and Rb atoms. We employed both a multireference configuration interaction approach and a full configuration interaction approach to obtain turning points, crossing points, potential minima, and spectroscopic molecular constants for the lowest five molecular states. Long-range parameters, including the dispersion coefficients are estimated from our *ab initio* data. We find a near degeneracy of the Yb$^+$ ground state with excited charge-transfer channels. The results for the long-range potential tail including the polarizability are seen to be in suitable agreement with previous experimental and theoretical work. We present preliminary results for the ultracold elastic scattering amplitude for the ytterbium ion colliding with the rubidium atom based on our *ab initio* data including both asymptotic ionic channels. These estimates, assuming pure adiabatic elastic scattering, indicate that the Yb$^+$ ion collisions with Rb atom interactions are attractive for both the singlet and triplet states. Effective range theory is used to derive the corresponding pseudopotential, which has a strong energy dependence, even in the nK regime not well represented by the single-parameter scattering length. The well-known sensitivity of the scattering length to changes in the potential indicates that our estimates are rather crude. Nonetheless, the potential-energy curves are accurate in the region where charge exchange is important and thus offer prospects of studying this process under quantum controlled conditions.

[1] C. J. Foot, *Atomic Physics* (Oxford University Press, Oxford, 2004).

[2] R. Côté and A. Dalgarno, Phys. Rev. A **58**, 498 (1998).

[3] A. Fioretti, D. Comparat, A. Crubellier, O. Dulieu, F. Masnou-Seeuws, and P. Pillet, Phys. Rev. Lett. **80**, 4402 (1998).

[4] W. C. Swalley and H. Wang, J. Mol. Spectrosc. **195**, 194 (1999).

[5] J. Weiner, V. Bagnato, S. Zilio, and P. S. Julienne, Rev. Mod. Phys. **71**, 1 (1999); G. H. Rawischer, B. D. Esry, E. Tiesinga, J. P. Burke, Jr., and I. Koltracht, J. Chem. Phys. **111**, 10418 (1999).

[6] L. Ratschbacher, C. Zipkes, C. Sias, and M. Köhl, Nat. Phys. (2012).

[7] A. T. Grier, M. Cetina, F. Oruevičević, and V. Vuletić, Phys. Rev. Lett. **102**, 223201 (2009); W. W. Smith, O. P. Makarov, and J. Lin, J. Mod. Opt. **52**, 2253 (2005).

[8] C. Zipkes, S. Palzer, L. Ratschbacher, C. Sias, and M. Köhl, Phys. Rev. Lett. **105**, 133201 (2010).

[9] C. Zipkes, S. Palzer, C. Sias, and M. Köhl, Nat. Lett. **464**, 388 (2010).

[10] Z. Idziaszek, T. Calarco, and P. Zoller, Phys. Rev. A **76**, 033409 (2007).

[11] R. Côté, V. Kharchenko, and M. D. Lukin, Phys. Rev. Lett. **89**, 093001 (2002).

[12] J. Goold, H. Doerk, Z. Idziaszek, T. Calarco, and T. Busch, Phys. Rev. A **81**, 041601(R) (2010).

[13] J. O. Hirshfelder, C. F. Curtiss, and R. B. Bird, *Molecular Theory of Gases and Liquids* (Wiley, New York, 1954).

[14] R. Côté and A. Dalgarno, Phys. Rev. A **62**, 012709 (2000).

[15] T. F. O'Malley, L. Spruch, and L. Rosenberg, J. Math. Phys. **2**, 491 (1961).

[16] Z. Idziaszek, T. Calarco, P. S. Julienne, and A. Simoni, Phys. Rev. A **79**, 010702(R) (2009).

[17] M. Krych, W. Skomorowski, F. Pawlowski, R. Moszynski, and Z. Idziaszek, Phys. Rev. A **83**, 032723 (2010).

[18] S. Schmid, A. Härter, and J. H. Denschlag, Phys. Rev. Lett. **105**, 133202 (2010).

[19] J. Mitroy, M. S. Safronova, and C. W. Clark, J. Phys. B **43**, 202001 (2010).

[20] I. S. Lim, M. Pernpointner, M. Seth, J. K. Laerdahl, P. Schwerdtfeger, P. Neogrady, and M. Urban, Phys. Rev. A **60**, 2822 (1999).

[21] R. W. Molof, H. L. Schwartz, T. M. Miller, and B. Bederson, Phys. Rev. A **10**, 1131 (1974).

[22] H. J. Werner *et al*., MOLPRO, version 2010.1, http://www.molpro.net.

[23] H. J. Werner and P. J. Knowles, J. Chem. Phys. **82**, 5053 (1985).

[24] P. J. Knowles and H. J. Werner, Chem. Phys. Lett. **115**, 259 (1985).

[25] H. J. Werner and P. J. Knowles, J. Chem. Phys. **89**, 5803 (1988).

[26] P. J. Knowles and H. J. Werner, Chem. Phys. Lett. **145**, 514 (1985).

[27] Y. Wang and M. Dolg, Theor. Chem. Acc. **100**, 124 (1998).

[28] L. von Szentpaly, P. Fuentealba, H. Preuss, and H. Stoll, Chem. Phys. Lett. **93**, 555 (1982).

[29] P. Fuentealba, H. Stoll, L. von. Szentpaly, P. Schwerdtfeger, and H. Preuss, J. Phys. B **16**, L323 (1983).

[30] E. R. Meyer and J. L. Bohn, Phys. Rev. A **80**, 042508 (2009).

[31] P. Camus, A. Débarre, and C. Morillon, J. Phys. B **13**, 1073 (1980).

[32] M. Aymar, A. Débarre, and O. Robaux, J. Phys. B **13**, 1089 (1980).

[33] W. F. Meggers and J. L. Tech, J. Res. Natl. Bur. Stand. (US) **83**, 13 (1978).

[34] I. Johansson, Ark. Fys. **20**, 135 (1961).

[35] R. J. Le Roy, University of Waterloo, Chemical Physics Research Report No. CP-663, 2007 (unpublished); see http://leroy.uwaterloo.ca/programs/.

[36] K. Huang, *Statistical Mechanics* (Wiley, New York, 1987).

[37] G. F. Gribakin and V. V. Flambaum, Phys. Rev. A **48**, 546 (1993).

[38] V. V. Flambaum, G. F. Gribakin, and C. Harabati, Phys. Rev. A **59**, 1998 (1999).

[39] V. A. Dzuba and A. Derevianko, J. Phys. B **43**, 074011 (2010).

[40] P. Zhang and A. Dalgarno, J. Phys. Chem. A **111**, 12471 (2007).

[41] X. Chu, A. Dalgarno, and G. C. Groenenboom, Phys. Rev. A **75**, 032723 (2007).

[42] A. Zangwill and P. Soven, Phys. Rev. A **21**, 1561 (1980).

[43] J. Mitroy and M. W. J. Bromley, Phys. Rev. A **68**, 052714 (2003).